Spaceflight alters bacterial gene expression and virulence and reveals role for global regulator Hfq

J.W. Wilson[1,2], C.M. Ott[3], K. Höner zu Bentrup[2], R. Ramamurthy[2], L. Quick[1], S. Porwollik[4], P. Cheng[4], M. McClelland[4], G. Tsaprailis[5], T. Radabaugh[5], A. Hunt[5], D. Fernandez[1], E. Richter[1], M. Shah[6], M. Kilcoyne[6], L. Joshi[6], M. Nelman-Gonzalez[7], S. Hing[8], M. Parra[8], P. Dumars[8], K. Norwood[9], R. Bober[9], J. Devich[9], A. Ruggles[9], C. Goulart[10], M. Rupert[10], L. Stodieck[10], P. Stafford[11], L. Catella[9], M.J. Schurr[2,12], K. Buchanan[2,13], L. Morici[2], J. McCracken[2,14], P. Allen[2,15], C. Baker-Coleman[2,15], T. Hammond[2,15], J. Vogel[16], R. Nelson[17], D.L. Pierson[3], H.M. Stefanyshyn-Piper[18], C.A. Nickerson[1,2]*

[1]The Biodesign Institute, Center for Infectious Diseases and Vaccinology, Arizona State University, Tempe, AZ; [2]Tulane University Health Sciences Center, New Orleans, LA; [3]Habitability and Environmental Factors Division, NASA-Johnson Space Center, Houston, TX; [4]Sidney Kimmel Cancer Center, San Diego, CA; [5]Center for Toxicology, University of Arizona, Tucson, AZ; [6]The Biodesign Institute, Center for Glycoscience Technology, Arizona State University, Tempe, AZ; [7]Wyle Laboratories, Houston, TX; [8]NASA-Ames Research Center, Moffett Field, CA; [9]Space Life Sciences Lab, Kennedy Space Center, Cape Canaveral, FL; [10]BioServe, University of Colorado, Boulder, CO; [11]The Biodesign Institute, Center for Innovations in Medicine, Arizona State University, Tempe, AZ; [12]University of Colorado at Denver and Health Science Center, Denver, CO; [13]Oklahoma City University, Oklahoma City, OK; [14]Section of General Surgery, University of Chicago, Chicago, IL; [15]Southeast Louisiana Veterans Health Care System, New Orleans, LA; [16]Max Planck Institute for Infection Biology,

RNA Biology Group, Berlin, Germany; [17]The Biodesign Institute, Center for Combinatorial Sciences, Arizona State University, Tempe, AZ; [18]Astronaut Office, NASA-Johnson Space Center, Houston, TX

***Corresponding author:** The Biodesign Institute, Center for Infectious Diseases and Vaccinology, Arizona State University, 1001 S. McAllister Avenue, Tempe, AZ 85287; phone: 480-727-7520; fax: 480-727-8943

One sentence summary: Spaceflight molecular microbiology reveals a role for the conserved Hfq regulatory network in the bacterial response to this environment.

Abstract

A comprehensive analysis of both the molecular genetic and phenotypic responses of any organism to the spaceflight environment has never been accomplished due to significant technological and logistical hurdles. Moreover, the effects of spaceflight on microbial pathogenicity and associated infectious disease risks have not been studied. The bacterial pathogen *Salmonella typhimurium* was grown aboard Space Shuttle mission STS-115 and compared to identical ground control cultures. Global microarray and proteomic analyses revealed 167 transcripts and 73 proteins changed expression with the conserved RNA-binding protein Hfq identified as a likely global regulator involved in the response to this environment. Hfq involvement was confirmed with a ground based microgravity culture model. Spaceflight samples exhibited enhanced virulence in a murine infection model and extracellular matrix accumulation consistent with a biofilm. Strategies to target Hfq and related regulators could potentially decrease infectious disease risks during spaceflight missions and provide novel therapeutic options on Earth.

Text

Environmental conditions and crewmember immune dysfunction associated with spaceflight may increase the risk of infectious disease during a long-duration mission (*1-4*). However, our knowledge of microbial changes in response to spaceflight conditions and the corresponding changes to infectious disease risk is limited and unclear. Elucidation of such risks and the mechanisms behind any spaceflight-induced changes to microbial pathogens holds the potential to decrease risk for human exploration of space and provide insight into how pathogens cause infections in Earth-based environments. Numerous logistical and technological hurdles exist when performing biological spaceflight experimentation, and an extremely limited number of opportunities to perform such research are available. Accordingly, comprehensive analysis of cells, including pathogenic microbes, at the molecular and phenotypic level during spaceflight offers a rare opportunity to examine their behavior and response in this environment.

We designed experiments to be flown on Space Shuttle Atlantis Mission STS-115 (September 2006) in which cultures of the bacterial pathogen *Salmonella typhimurium* were activated to grow in space for a specific time period and then either fixed in an RNA/protein fixative or supplemented with additional growth media after this time period (Supplemental Figure 1, Panel A). Immediately upon landing at Kennedy Space Center (KSC), the culture samples were recovered and subsequently used for whole-genome transcriptional microarray and proteomic analysis (fixed samples) or for infections in a murine model of salmonellosis (media-supplemented samples). In each case, the flight culture samples were compared to culture samples grown under identical conditions on the ground at KSC using coordinated activation and termination times (via real time communications with the Shuttle crew) in an insulated room that

maintained the identical temperature and humidity as that on the Shuttle (Orbital Environment Simulator or OES). The culture experiments were loaded into specially-designed hardware (termed fluid processing apparatus or FPA) to facilitate controlled activation and fixation of the cultures while maintaining suitable culture containment requirements (Supplemental Figure 1, Panels B,C).

To determine which genes changed expression in response to spaceflight, total bacterial RNA was isolated from the fixed flight and ground samples, qualitatively analyzed to ensure lack of degradation, quantitated, and then reversed transcribed into labeled, single-stranded cDNA. The labeled cDNA was co-hybridized with differentially-labeled *S. typhimurium* genomic DNA to whole genome *S. typhimurium* microarray slides. The cDNA signal hybridizing to each gene spot was quantitated, and the normalized, background-subtracted data was analyzed for statistically-significant, 2-fold or greater differences in gene expression between the flight and ground samples. We found 167 genes differentially-expressed in flight as compared to ground from a variety of functional categories (69 up-regulated and 98 down-regulated) (Supplemental Table 1). The proteomes of fixed cultures were also obtained via multi-dimensional protein identification (MudPIT) analysis. We identified 251 proteins expressed in the flight and ground cultures, with 73 being present at different levels in these samples (Supplemental Table 2). Several of the genes encoding these proteins were also identified via microarray analysis. Collectively, these gene expression changes form the first documented bacterial spaceflight stimulon indicating that bacteria respond to this environment with widespread alterations of expression of genes distributed globally throughout the chromosome (Figure 1, Panel A).

Identification of one or more regulators of the spaceflight stimulon represents an important step in understanding the nature of this unique environmental signal. Our data indicated that a pathway involving the conserved RNA-binding regulatory protein Hfq played a role in this response (Table 1). Hfq is an RNA chaperone that binds to small regulatory RNA and mRNA molecules to facilitate mRNA translational regulation in response to periplasmic stress (in conjuction with the specialized sigma factor RpoE), environmental stress (via alteration of RpoS expression), and changes in metabolite concentrations, such as iron levels (via the Fur pathway) (*5-9*). Hfq is also involved in promoting the virulence of several pathogens including *S. typhimurium (10)*, and Hfq homologues are highly conserved across species of prokaryotes and eukaryotes (*11*). Our data strongly supported a role for Hfq in the response to spaceflight: (1) The expression of *hfq* was decreased in flight, and this finding matched previous results in which *S. typhimurium hfq* gene expression was decreased in a ground-based model of microgravity (*12*); (2) Expression of 64 genes in the Hfq regulon was altered in flight (32% of the total genes identified), and the directions of differential changes of major classes of these genes matched predictions associated with decreased *hfq* expression (see subsequent examples); (3) several small regulatory RNAs that interact with Hfq were differentially regulated in flight as would be predicted if small RNA/Hfq pathways are involved in a spaceflight response; (4) The levels of OmpA, OmpC, and OmpD mRNA and protein are classic indicators of the RpoE-mediated periplasmic stress response which involves Hfq (*13*). Transcripts encoding OmpA, OmpC, and OmpD (and OmpC protein level) were up-regulated in flight, correlating with *hfq* down-regulation; (5) Hfq promotes expression of a large class of ribosomal structural protein genes (*9*), and we found many such genes exhibited decreased expression in flight; (6) Hfq is a negative regulator of the large *tra* operon encoding the F plasmid transfer apparatus (*14*), and

several *tra* genes from related operons on two plasmids present in *S. typhimurium* χ3339 were up regulated in flight; (7) Hfq is intimately involved in a periplasmic stress signaling pathway that is dependent on the activity levels of three key proteins, RpoE, DksA, and RseB (*5, 9*). Differential expression of these genes was observed in flight; (8) Hfq regulates the expression of the Fur protein and other genes involved in the iron response pathway (*6, 8*). We observed several iron utilization/storage genes with altered expression in flight. This finding also matched previous results in which iron pathway genes changed expression in a ground-based model of microgravity, and the Fur protein was shown to play a role in stress resistance alterations induced in the same model (*12*).

Given these findings, we designed experiments to verify a role for Hfq in the spaceflight response using a cellular growth apparatus that serves as a ground-based model of microgravity conditions termed the rotating wall vessel (RWV). Designed by NASA, the RWV has been extensively used in this capacity to study the effects of a low fluid shear growth environment (which closely models the liquid growth environment encountered by cells in microgravity) on various types of cells (*15-18*). Studies with the RWV involve using two separate apparatus: one is operated in the modeled microgravity position (termed low-shear modeled microgravity or LSMMG) and one is operated as a control in a position (termed 1xg) where sedimentation due to gravity is not offset by the rotating action of the vessel.

LSMMG-induced alterations in acid stress resistance and macrophage survival of *S. typhimurium* have previously been shown to be associated with global changes in gene expression and virulence (*12, 19*). We grew wild type and isogenic *hfq* mutant strains of *S. typhimurium* in the RWV in the LSMMG and 1xg positions and assayed the acid stress response and macrophage survival of these cultures. While the wild type strain displayed a significant

difference in acid resistance between the LSMMG and 1xg cultures, this response was not observed in the *hfq* mutant, which contains a deletion of the *hfq* gene and replacement with a Cm-r cassette (Figure 2, Panel A). Two control strains, *hfq* 3'Cm and *invA* Km, gave the same result as the WT strain. We also observed increased intracellular replication of the LSMMG-grown WT (*hfq* 3'Cm) strain in infected J774 macrophages as compared to the 1xg control, and this phenotype was not observed in the *hfq* mutant strain (Figure 2, Panel B). Collectively, these data indicate that Hfq is involved in the bacterial spaceflight response as confirmed in a ground-based model of microgravity conditions. In addition, the intracellular replication phenotype inside macrophages correlates with the finding that spaceflight and LSMMG cultures exhibit increased virulence in mice (see text below and reference (*19*)).

Since growth during spaceflight and potential global reprogramming of gene expression in response to this environment could alter the virulence of a pathogen, we compared the virulence of *S. typhimurium* spaceflight samples to identical ground controls as a second major part of our study. Bacteria from flight and ground cultures were harvested and immediately used to inoculate female Balb/c mice via a per-oral route of infection on the same day as landing. Two sets of mice were infected at increasing dosages of either flight or ground cultures, and the health of the mice was monitored every 6-12 hours for 30 days. Mice infected with bacteria from the flight cultures displayed a decreased time to death (at the 10^7 dosage), increased percent mortality at each infection dosage and a decreased LD_{50} value compared to those infected with ground controls (Figure 2, Panels B,C,D). These data indicated increased virulence for spaceflight *S. typhimurium* samples and are consistent with previous studies in which the same strain of *S. typhimurium* grown using LSMMG conditions displayed enhanced virulence in a murine model as compared to 1xg controls (*19*).

To determine any morphological differences between flight and ground cultures, scanning electron microscopic (SEM) analysis of bacteria from these samples was performed. While no difference in the size and shape of individual cells in both cultures was apparent, the flight samples demonstrated clear differences in cellular aggregation and clumping that was associated with the formation of an extracellular matrix (Figure 2, Panel E). Consistent with this finding, several genes associated with surface alterations related to biofilm formation changed expression in flight (up-regulation of *wca/wza* colonic acid synthesis operon, *ompA, fimH;* down-regulation of motility genes) (Table 1). SEM images of other bacterial biofilms show a similar matrix accumulation (*20, 21*). This phenotype indicates a change in bacterial community potentially related to the increased virulence of the flight bacteria in the murine model.

These results present the first documented gene expression changes that occur in bacterial cells (and any microbial pathogen) during spaceflight and therefore demonstrate that a microgravity growth environment represents a *bona fide* signal that can induce molecular changes in bacterial cells. These results also provide the first direct evidence that growth during spaceflight can alter the virulence of pathogen; in this case, a bacterial pathogen grown in spaceflight displayed increased virulence in a murine model of infection. Strategies designed to counteract the virulence-enhancing effects of spaceflight in microbes provide important potential benefits to crew health and open insight into novel antimicrobial strategies on Earth. The identification of global regulators of these responses such as Hfq provides targets at which these strategies can be directed.

References

1. A. I. Grigoriev, E. N. Svetaylo, A. D. Egorov, *Environ Med* **42**, 83 (Dec, 1998).
2. G. Sonnenfeld, W. T. Shearer, *Nutrition* **18**, 899 (Oct, 2002).
3. G. R. Taylor, *J Leukoc Biol* **54**, 202 (Sep, 1993).
4. G. R. Taylor, I. Konstantinova, G. Sonnenfeld, R. Jennings, *Adv Space Biol Med* **6**, 1 (1997).
5. N. Figueroa-Bossi *et al.*, *Mol Microbiol* **62**, 838 (Nov, 2006).
6. E. Masse, S. Gottesman, *Proc Natl Acad Sci U S A* **99**, 4620 (Apr 2, 2002).
7. A. Muffler, D. D. Traulsen, D. Fischer, R. Lange, R. Hengge-Aronis, *J Bacteriol* **179**, 297 (Jan, 1997).
8. B. Vecerek, I. Moll, T. Afonyushkin, V. Kaberdin, U. Blasi, *Mol Microbiol* **50**, 897 (Nov, 2003).
9. E. Guisbert, V. A. Rhodius, N. Ahuja, E. Witkin, C. A. Gross, *J Bacteriol* **189**, 1963 (Mar, 2007).
10. A. Sittka, V. Pfeiffer, K. Tedin, J. Vogel, *Mol Microbiol* **63**, 193 (Jan, 2007).
11. P. Valentin-Hansen, M. Eriksen, C. Udesen, *Mol Microbiol* **51**, 1525 (Mar, 2004).
12. J. W. Wilson *et al.*, *Proc Natl Acad Sci U S A* **99**, 13807 (Oct 15, 2002).
13. P. Valentin-Hansen, J. Johansen, A. A. Rasmussen, *Curr Opin Microbiol* **10**, 152 (Apr, 2007).
14. W. R. Will, L. S. Frost, *J Bacteriol* **188**, 124 (Jan, 2006).
15. T. G. Hammond, J. M. Hammond, *Am J Physiol Renal Physiol* **281**, F12 (Jul, 2001).
16. C. A. Nickerson, C. M. Ott, *ASM News* **70**, 169 (2004).
17. C. A. Nickerson *et al.*, *J Microbiol Methods* **54**, 1 (Jul, 2003).
18. C. A. Nickerson, C. M. Ott, J. W. Wilson, R. Ramamurthy, D. L. Pierson, *Microbiol Mol Biol Rev* **68**, 345 (Jun, 2004).
19. C. A. Nickerson *et al.*, *Infect Immun* **68**, 3147 (Jun, 2000).
20. B. Little, P. Wagner, R. Ray, R. Pope, R. Scheetz, *J Ind Microbiol* **8**, 213 (1991).
21. J. H. Priester *et al.*, *J Microbiol Methods* **68**, 577 (Mar, 2007).
22. L. J. Reed, H. Muench, *Am J Hyg* **27**, 493 (1938).

23. Acknowledgments: All supporting team members at Kennedy Space Center, Johnson Space Center, Ames Research Center, Marshall Spaceflight Center, and BioServe Space Technologies; the Crew of STS-115; Neal Pellis; Roy Curtiss III; Marc Porter; Lucy Shapiro; Brian Haight; Shawn Watts; Michael Caplan; Joseph Caspermeyer; Clint Coleman; Charles Arntzen; and all of our family and friends for their support. This work was supported by NASA grant NCC2-1362 to CAN; Louisiana Board of Regents grant NNG05GH22H to CBC; Arizona Proteomics Consortium supported by NIEHS grant ES06694 to the SWEHSC, NIH/NCI grant CA023074 to the AZCC, and by the BIO5 Institute of the University of Arizona.

Figure legends

Figure 1. Data from STS-115 *Salmonella typhimurium* experiments. Panel A: Map of the 4.8 Mb circular *Salmonella typhimurium* genome with the locations of the genes belonging to the spaceflight transcriptional stimulon indicated as black hatch marks. Panel B: Decreased time-to-death in mice infected with flight *S. typhimurium* as compared to identical ground controls. Female Balb/c mice perorally infected with 10^7 bacteria from either spaceflight or ground cultures were monitored every 6-12 hours over a 30 day period and the percent survival of the mice in each group was graphed versus number of days. Panel C: Increased percent mortality of mice infected with spaceflight cultures across a range of infection dosages. Groups of mice were infected with increasing dosages of bacteria from spaceflight and ground cultures and monitored for survival over 30 days. The percent mortality (calculated as in (*22*)) of each dosage group is graphed versus the dosage amount. Panel D: Decreased LD_{50} value (calculated as in (*22*)) for spaceflight bacteria in murine infection model. Panel E: Scanning electron microscopy (3500X magnification) of spaceflight and ground *S. typhimurium* bacteria showing the formation of an extracellular matrix and associated cellular aggregation of spaceflight cells.

Figure 2. Hfq is required for *S. typhimurium* LSMMG-induced phenotypes in RWV culture. Panel A: The survival ratio of wild type and isogenic *hfq, hfq* 3' Cm, and *invA* mutant strains in acid stress after RWV culture in the LSMMG and 1xg positions is plotted (p-value < 0.05).

Panel B: Fold intracellular replication of *S. typhimurium* strains *hfq* 3'Cm and Δ*hfq* in J774 macrophages after RWV culture as above. Intracellular bacteria were quantitated at 2 hours and 24 hours post-infection, and the fold increase in bacterial numbers between those two time periods was calculated (p-value < 0.05).

Figure 1.

A.

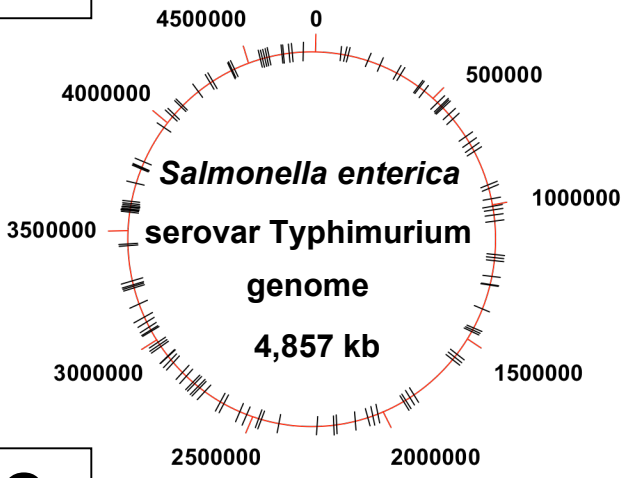

B.

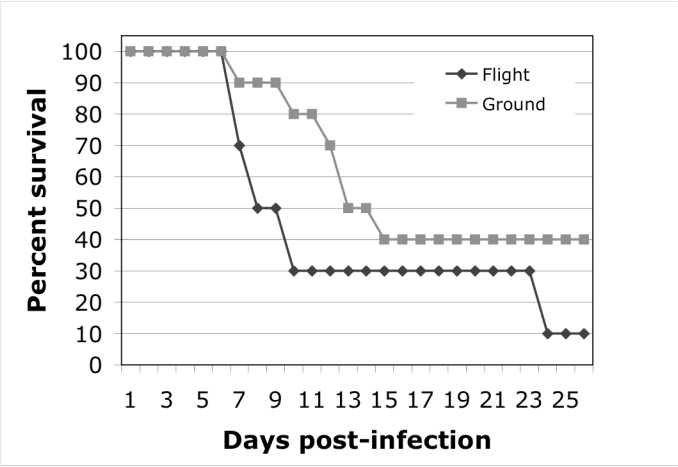

C.

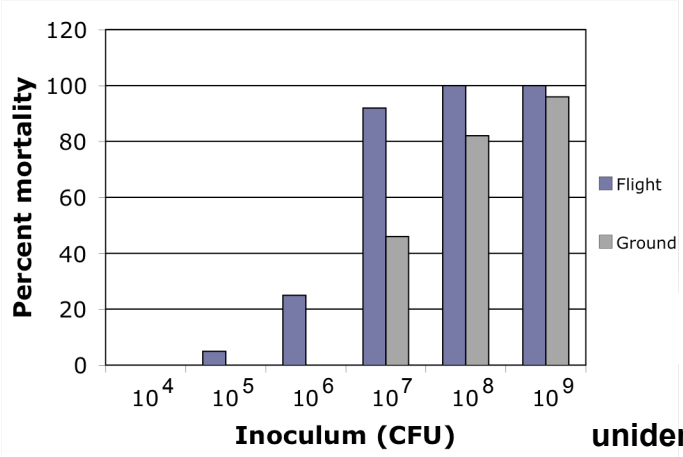

D.

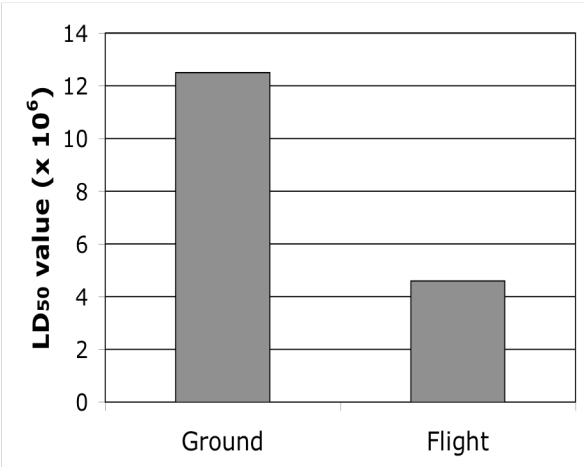

E.

Flight

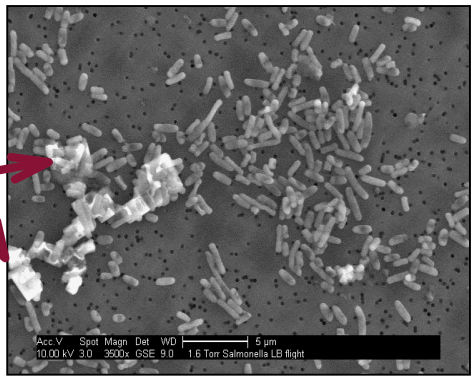

Ground

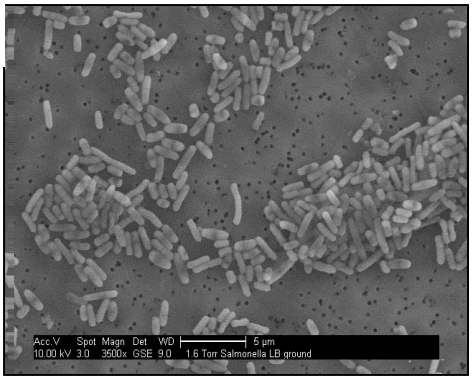

Figure 2.

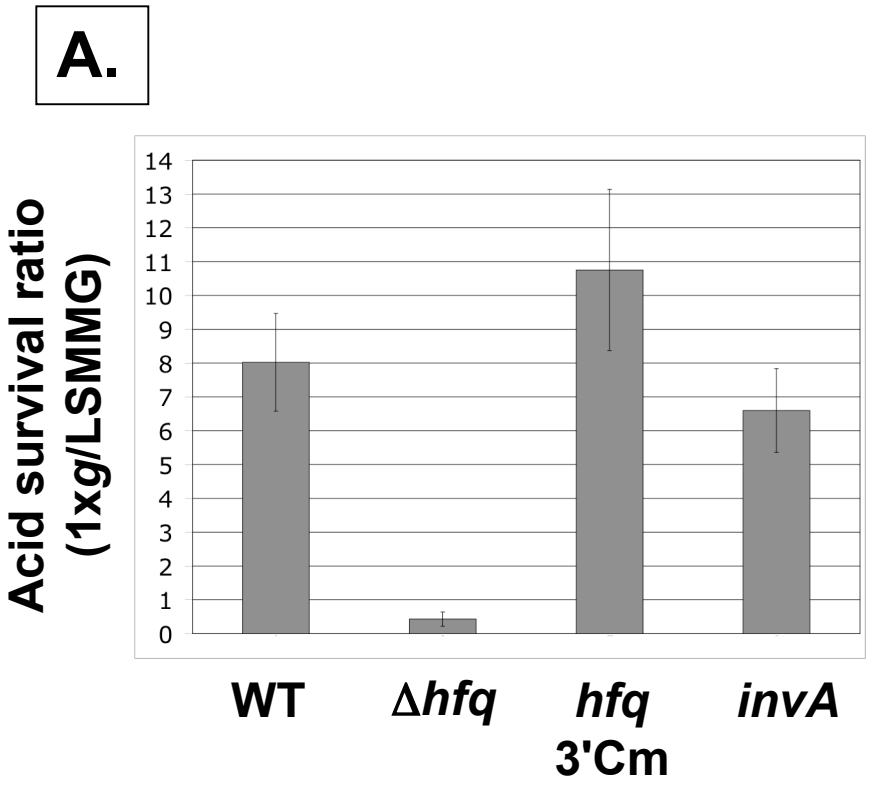
A.
Acid survival ratio
(1xg/LSMMG)
14
13
12
11
10
9
8
7
6
5
4
3
2
1
0
WT
ΔhfqΔ
hfq
3'Cm
invA

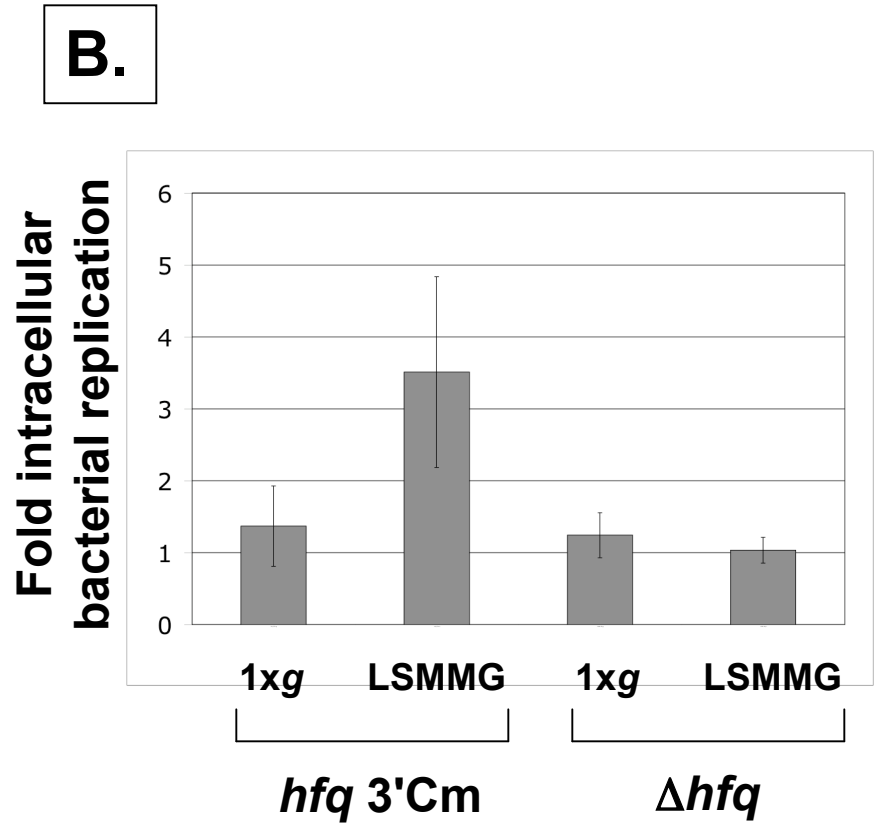
B.
Fold intracellular
bacterial replication
6
5
4
3
2
1
0
1xg
LSMMG
1xg
LSMMG
hfq 3'Cm
ΔhfqΔ

Table 1: Spaceflight stimulon genes belonging to Hfq regulon or involved with iron utilization or biofilm formation

Gene*	Fold change	Function
Hfq regulon genes		
Up-regulated		
Outer membrane proteins		
ompA	2.05	outer membrane porin
ompC	2.44	outer membrane porin
ompD	3.34	outer membrane porin
Plasmid transfer apparatus		
traB	4.71	conjugative transfer, assembly
traN	4.24	conjugative transfer, aggregate formation
trbA	3.14	conjugative transfer
traK	2.91	conjugative transfer
traD	2.87	conjugative transfer, DNA transport
trbC	2.68	conjugative transfer
traH	2.59	conjugative transfer, assembly
traX	2.37	conjugative transfer, fimbrial acetylation
traT	2.34	conjugative transfer
trbB	2.32	conjugative transfer
traG	2.21	conjugative transfer, assembly
traF	2.11	conjugative transfer
traR	1.79	conjugative transfer
Various cellular functions		
gapA	7.67	glyceraldehyde-3-phosphate dehydrogenase A
sipC	6.27	cell invasion protein
adhE	4.75	iron-dependent alcohol dehydrogenase of AdhE
glpQ	2.58	glycerophosphodiester phosphodiesterase, periplasmic
fliC	2.11	flagellin, filament structural protein
sbmA	1.67	putative ABC superfamily transporter
Down-regulated		
Small RNAs		
alpha RBS	0.305	small RNA
rnaseP	0.306	small RNA regulatory
csrB	0.318	small RNA regulatory
tke1	0.427	small RNA
oxyS	0.432	small RNA regulatory
RFN	0.458	small RNA
rne5	0.499	small RNA
Ribosomal proteins		
rpsL	0.251	30S ribosomal subunit protein S12
rpsS	0.289	30S ribosomal subunit protein S19
rplD	0.393	50S ribosomal subunit protein L4
rpsF	0.401	30S ribosomal subunit protein S6
rplP	0.422	50S ribosomal subunit protein L16
rplA	0.423	50S ribosomal subunit protein L1
rpme2	0.473	50S ribosomal protein L31 (second copy)
rplY	0.551	50S ribosomal subunit protein L25

Various cellular functions

ynaF	0.201	putative universal stress protein
ygfE	0.248	putative cytoplasmic protein
dps	0.273	stress response DNA-binding protein
hfq	0.298	host factor for phage replication, RNA chaperone
osmY	0.318	hyperosmotically inducible periplasmic protein
mysB	0.341	suppresses protein export mutants
rpoE	0.403	sigma E (sigma 24) factor of RNA polymerase
cspD	0.421	similar to CspA but not cold shock induced
nlpb	0.435	lipoprotein-34
ygaC	0.451	putative cytoplasmic protein
ygaM	0.453	putative inner membrane protein
gltI	0.479	ABC superfamily, glutamate/aspartate transporter
ppiB	0.482	peptidyl-prolyl cis-trans isomerase B (rotamase B)
atpE	0.482	membrane-bound ATP synthase, F0 sector, subunit c
yfiA	0.482	ribosome associated factor, stabilizes against dissociation
trxA	0.493	thioredoxin 1, redox factor
nifU	0.496	NifU homologs involved in Fe-S cluster formation
rbfA	0.506	ribosome-binding factor, role in processing of 10S rRNA
rseB	0.514	anti-sigma E factor
yiaG	0.528	putative transcriptional regulator
ompX	0.547	outer membrane protease, receptor for phage OX2
rnpA	0.554	RNase P, protein component (protein C5)
hns	0.554	DNA-binding protein; pleiotropic regulator
lamB	0.566	phage lambda receptor protein; maltose high-affinity receptor
rmf	0.566	ribosome modulation factor
tpx	0.566	thiol peroxidase
priB	0.571	primosomal replication protein N

Iron utilization/storage genes

adhE	4.76	iron-dependent alcohol dehydrogenase of AdhE
entE	2.24	2,3-dihydroxybenzoate-AMP ligase
hydN	2.03	electron transport protein (FeS senter) from formate to hydrogen
dmsC	0.497	anaerobic dimethyl sulfoxide reductase, subunit C
nifU	0.495	NifU homologs involved in Fe-S cluster formation
fnr	0.494	transcriptional regulator, iron-binding
fdnH	0.458	formate dehydrogenase-N, Fe-S beta subunit, nitrate-inducible
frdC	0.411	fumarate reductase, anaerobic, membrane anchor polypeptide
bfr	0.404	bacterioferrin, an iron storage homoprotein
ompW	0.276	outer membrane protein W; colicin S4 receptor
dps	0.273	stress response DNA-binding protein and ferritin

Genes implicated in/associated with biofilm formation

wza	2.30	putative polysaccharide export protein, outer membrane
wcaI	2.07	putative glycosyl transferase in colanic acid biosynthesis
ompA	2.06	outer membrane protein
wcaD	1.82	putative colanic acid polymerase
wcaH	1.76	GDP-mannose mannosyl hydrolase in colanic acid biosynthesis
manC	1.71	mannose-1-phosphate guanylyltransferase
wcaG	1.68	bifunctional GDP fucose synthetase in colanic acid biosyntheis
wcaB	1.64	putative acyl transferase in colanic acid biosynthesis
fimH	1.61	fimbrial subunit
fliS	0.339	flagellar biosynthesis

flgM	0.343	flagellar biosynthesis
flhD	0.356	flagellar biosynthesis
fliE	0.438	flagellar biosynthesis
fliT	0.444	flagellar biosynthesis
cheY	0.461	chemotaxic response
cheZ	0.535	chemotaxic response

*For specific parameters used to identify these genes, please refer to Materials and Methods in the Supplementary Material.

Supplemental Material

Materials and Methods

Strains, media, and chemical reagents

The virulent, mouse-passaged *Salmonella typhimurium* derivative of SL1344 termed χ3339 was used as the wild type strain in all flight and ground-based experiments (*1*). Isogenic derivatives of SL1344 with mutations Δ*hfq*, *hfq* 3'Cm, and *invA* Km were used in ground-based experiments (*2, 3*). The Δ*hfq* strain contains a deletion of the *hfq* open reading frame (ORF) and replacement with a chloramphenicol resistance cassette, and the *hfq* 3'Cm strain contains an insertion of the same cassette immediately downstream of the WT *hfq* ORF. The *invA* Km strain contains a kanamycin resistance cassette inserted in the *invA* ORF. Lennox broth (LB) was used as the growth media in all experiments (*4*) and phosphate buffered saline (PBS) (Invitrogen, Carlsbad, CA) was used to resuspend bacteria for use as inoculum in the FPAs. The RNA fixative RNA Later II (Ambion, Austin, TX), glutaraldehyde (16%) (Sigma, St. Louis, MO), and formaldehyde (2%) (Ted Pella Inc., Redding, CA) were used as fixatives in flight experiments.

Loading of fluid processing apparatus (FPA)

An FPA consists of a glass barrel that can be divided into compartments via the insertion of rubber stoppers and a lexan sheath into which the glass barrel is inserted (refer to Supplemental Figure 1). Each compartment in the glass barrel was filled with a solution in an order such that the solutions would be mixed at specific timepoints in flight via two actions: (1) downward plunging action on the rubber stoppers and (2) passage of the fluid in a given compartment through a bevel on the side of the glass barrel such that it was

released into the compartment below. Glass barrels and rubber stoppers were coated with a silicone lubricant (Sigmacote, Sigma, St. Louis, MO) and autoclave separately before assembly. A stopper with a gas exchange membrane was inserted just below the bevel in the glass barrel before autoclaving. FPA assembly was performed aseptically in a laminar flow hood in the following order: 2.0 ml LB media on top of the gas exchange stopper, one rubber stopper, 0.5 ml PBS containing bacterial inoculum (approximately 6.7 $x10^6$ bacteria), another rubber stopper, 2.5 ml of either RNA fixative or LB media, and a final rubber stopper. Syringe needles (gauge 25 5/8) were inserted into rubber stoppers during this process to release air pressure and facilitate assembly. To facilitate group activation of FPAs during flight and to ensure proper containment levels, sets of 8 FPAs were loaded into larger containers termed group activation packs (GAPs).

Murine infection assay

Six to eight week old female Balb/c mice (housed at the Space Life Sciences Lab at Kennedy Space Center) were fasted for approximately 6 hours and then per-orally infected with increasing dosages of *S. typhimurium* harvested from flight and ground FPA cultures and resuspended in buffer saline gelatin (*5*). Ten mice per infectious dosage were used, and food and water were returned to the animals within 30 minutes post-infection. The infected mice were monitored every 6-12 hours for 30 days. The LD_{50} value was calculated using the formula of Reed and Muench (*6*).

Scanning electon microscopy

A portion of cells from the viable, media-supplemented cultures from flight and ground FPAs were fixed for scanning electron microscopic analysis using 8% glutaraldehyde and 1% formaldehyde and were processed for SEM as described previously (*7*).

Microarray analysis

Total cellular RNA purification, preparation of fluorescently-labeled, single stranded cDNA probes, probe hybridization to whole genome *S. typhimurium* microarrays, and image acquisition was performed as previously described (*8*) using three biological and three technical replicates for each culture condition. Flow cytometric analysis revealed that cell numbers in flight and ground biological replicate cultures were not statistically different. Data from stored array images were obtained via QuantArray software (Packard Bioscience, Billerica, MA) and statistically analyzed for significant gene expression differences using the Webarray suite as described previously (*9*). GeneSpring software was also used to validate the genes identified with the Webarray suite. To obtain the genes comprising the spaceflight stimulon as listed in Supplemental Table 1, the following parameters were used in Webarray: a fold increase or decrease in expression of 2 fold or greater, a spot quality (A-value) of greater than 9.5, and p-value of less than 0.05. For some genes listed in Table 1, the following parameters were used: a fold increase or decrease in expression of value greater than 1.6 or less then 0.6 respectively, an A-value of 8.5 or greater, and p-value of less then 0.1. The vast majority of genes listed in Table 1 had an A-value of greater than 9.0 (with most being greater than 9.5) and a p-value of 0.05 or less. The exceptions were as follows: *sbmA* (p-value=0.06), *oxyS* (A-value=8.81), *rplY* (A-value=8.95), *cspD* (A-value=8.90), *yfiA* (p-value=0.08), *ompX* (p-value=0.09), *hns* (p-value=0.08), *rmf* (A-value=8.82), *wcaD* (p-value 0.09), and *fliE* (A-value=8.98). To identify spaceflight stimulon genes also contained in the Hfq regulon, proteins or genes found to be regulated by Hfq or RNAs found to be bound by Hfq as reported in the indicated references were scanned against

the spaceflight microarray data for expression changes within the parameters above (*2, 10-13*).

Multidimensional protein identification (MudPIT) analysis via tandem mass spectrometry coupled to dual nano-liquid chromatography (LC-LC-MS/MS)

Acetone-protein precipitates from whole cell lysates obtained from flight and ground cultures (representing three biological replicates) were re-suspended in water and assayed for amount using a BioRad Model 680 microplate reader according to published procedures (*14, 15*). Eighteen μg of total protein from the whole cell lysate samples was digested in triplicate with trypsin (10 μg/mL) at 37^{o}C overnight following reduction with dithiothreitol and alkylation with iodoacetamide (*16*). For the nano LC-LC-MS/MS, a microbore HPLC system (Paradigm MS4, Michrom, Auburn, CA) was used with two separate strong cation exchange (SCX) and reversed phase (RP) columns: a 100 μm I.D. capillary packed with 7 cm of 5 μm Vydac C18 reversed phase resin and a separate 250 μm I.D. capillary packed with 7cm of 5 μm Partisphere strong cation exchanger resin (Whatman, Clifton, NJ). The samples (18 μg) (representing three technical replicates) were acidified using TFA and manually injected onto the SCX column, the effluent from the column being fed through RP column. A representative twelve step LC-LC-MS/MS analysis would be as follows. Solutions used are: 10% methanol/0.1% formic acid, 0.01%TFA (buffer A), 95% methanol/0.1% formic acid, 0.01% TFA (buffer B), 10% methanol/0.1% formic acid, 0.01% TFA (buffer C) and 500 mM ammonium acetate/10% methanol/0.1% formic acid, 0.01% TFA (buffer D). Step 1 consists of a 5 min equilibration step at 100% buffer A, followed by another equilibration step for 5 min at 25% buffer B (75% buffer A), followed by a 40 min gradient from 25% buffer B to 65%

buffer B, followed by a 10 min 65% buffer B and 10 min of 100% buffer A. Chromatography steps 2 to 12 follow the same pattern: 15 min of the appropriate % of buffers C & D followed by a 2 min 100% buffer C wash, a 5 min wash with 100% A, equilibration with 25% buffer B for 5 min, followed by a gradient from 25% buffer B to 65% buffer B in 40 min, followed by a 10 min 65% buffer B and 10 min of 100% buffer A. The buffer C/D percentages used were 95/5%, 90/10%, 85/15%, 80/20%, 70/30%, 60/40%, 40/60%, 20/80%, 0/100%, 0/100%, 0/100% respectively, for the 11 salt steps. The flow rate was approximately 350 nl/min, with elution directly into a custom built nanoelectrospray ionization source of a ThermoFinnigan LCQ-Deca XP Plus ion trap mass spectrometer (ThermoFinnigan, San Jose, CA). Dependent data scanning was performed by Xcalibur v 1.4 software (*17*) with a default charge of 2, an isolation width of 1.5 amu, an activation amplitude of 35%, activation time of 30 msec, and a minimal signal of 10000 ion counts. Global dependent data settings were as follows, reject mass width of 1.5 amu, dynamic exclusion enabled, exclusion mass width of 1.5 amu, repeat count of 1, repeat duration of 1 min, and exclusion duration of 5 min. Scan event series included one full scan with mass range 380 – 2000 Da, followed by 3 dependent MS/MS scan of the most intense ion. Tandem MS spectra of peptides were analyzed with TurboSEQUEST™ v 3.1, a program that allows the correlation of experimental tandem MS data with theoretical spectra generated from known protein sequences (*18*). The peak list (dta files) for the search were generated by Bioworks 3.1. Parent peptide mass error tolerance was set at 1.5 amu and fragment ion mass tolerance was set at 0.5 amu during the search. The criteria that were used for a preliminary positive peptide identification are the same as previously described, namely peptide precursor ions with a +1 charge having

a Xcorr >1.8, +2 Xcorr > 2.5 and +3 Xcorr > 3.5. A dCn score > 0.08 and a fragment ion ratio of experimental/theorical >50% were also used as filtering criteria for reliable matched peptide identification (*19, 20*). All matched peptides were confirmed by visual examination of the spectra. All spectra were searched against a *Salmonella typhimurim* database created from the latest version of the non-redundant protein database downloaded July 7, 2006 from NCBI. At the time of the search this *Salmonella typhimurim* database contained 11,970 entries. The results were also validated using XTandem, another search engine (*21*), and with Scaffold, a program that relies on various search engine results (ie: Sequest, XTandem, MASCOT) and which uses Bayesian statistics to reliably identify more spectra (*22, 23*). Please refer to Supplementary Table 2 for the specific parameters used in Scaffold to identify the proteins in this study.

Ground-based RWV cultures and acid stress and macrophage survival assays

S. typhimurium cultures were grown in rotating wall vessels in the LSMMG and 1xg orientations and assayed for resistance to pH=3.5 and survival inside J774 macrophages as described previously (*5*), except that the RWV cultures were grown for 24 hours at 37 degrees C. For acid stress assays, the percentage of surviving bacteria present after 45-60 minutes acid stress (compared to the original number of bacteria before addition of the stress) was calculated. A ratio of the percent survival values for the LSMMG and 1xg cultures was obtained (indicating the fold difference in survival between these cultures) and is presented as the acid survival ratio in Figure 2 in the text. The mean and standard deviation from three independent experimental trials is presented. For macrophage survival assays, the number of bacteria present inside J774 macrophages at 2 hours and 24 hours post-infection was determined, and the fold difference between these two

numbers was calculated. The mean and standard deviation of values from three independent experimental trials (each done in triplicate tissue culture wells) is presented. The statistical differences observed in the graphs in Figure 2 were calculated at p-values less than 0.05.

Supplemental Figure Legend

Supplemental Figure 1. Experimental setup for STS-115 *Salmonella typhimurium* microarray and virulence experiments. Panel A: This flowchart displays a timeline of how the STS-115 experiment was designed and organized. Fluid processing apparatuses (FPAs) were loaded as in Panel B below and delivered to Shuttle, activated during spaceflight, and recovered upon landing as outlined in the flowchart. OES: Orbital Environmental Simulator. SLSL: Space Life Sciences Lab. Panel B: Photograph of loaded FPAs in pre-flight configuration. An FPA consists of a glass barrel that contains a short bevel on one side and stoppers inside that separate individual chambers containing fluids used in the experiment. The glass barrel loaded with stoppers and fluids is housed inside a lexan sheath containing a plunger that pushes on the top stopper to facilitate mixing of fluids at the bevel. The bottom stopper in the glass barrel (and also the bottom of the lexan sheath) is designed to contain a gas-permeable membrane that allows air exchange during bacterial growth. In the STS-115 experiment, the bottom chamber contained LB media, the middle chamber contained the bacterial inoculum suspended in PBS, and the top chamber contained either RNA/protein fixative or additional LB media. Upon activation, the plunger was pushed down so that only the middle chamber fluid was mixed with the bottom chamber to allow media inoculation and bacterial growth. After the 25 hour growth period, the plunger was pushed so that the top chamber fluid was added. Panel C: Photograph of FPAs in post-flight configuration showing that all stoppers have been pushed together and the entire fluid sample is in the bottom chamber.

Supplemental References

1. P. A. Gulig, R. Curtiss, 3rd, *Infect Immun* **55**, 2891 (Dec, 1987).
2. A. Sittka, V. Pfeiffer, K. Tedin, J. Vogel, *Mol Microbiol* **63**, 193 (Jan, 2007).
3. J. W. Wilson, C. A. Nickerson, *BMC Evol Biol* **6**, 2 (2006).
4. E. S. Lennox, *Virology* **1**, 190 (Jul, 1955).
5. C. A. Nickerson *et al.*, *Infect Immun* **68**, 3147 (Jun, 2000).
6. L. J. Reed, H. Muench, *Am J Hyg* **27**, 493 (1938).
7. C. A. Nickerson *et al.*, *Infect Immun* **69**, 7106 (Nov, 2001).
8. J. W. Wilson *et al.*, *Proc Natl Acad Sci U S A* **99**, 13807 (Oct 15, 2002).
9. W. W. Navarre *et al.*, *Science* **313**, 236 (Jul 14, 2006).
10. N. Figueroa-Bossi *et al.*, *Mol Microbiol* **62**, 838 (Nov, 2006).
11. E. Guisbert, V. A. Rhodius, N. Ahuja, E. Witkin, C. A. Gross, *J Bacteriol* **189**, 1963 (Mar, 2007).
12. W. R. Will, L. S. Frost, *J Bacteriol* **188**, 124 (Jan, 2006).
13. A. Zhang *et al.*, *Mol Microbiol* **50**, 1111 (Nov, 2003).
14. O. H. Lowry, N. J. Rosebrough, A. L. Farr, R. J. Randall, *J Biol Chem* **193**, 265 (Nov, 1951).
15. G. L. Peterson, *Anal Biochem* **100**, 201 (Dec, 1979).
16. A. Shevchenko, M. Wilm, O. Vorm, M. Mann, *Anal Chem* **68**, 850 (Mar 1, 1996).
17. N. L. Andon *et al.*, *Proteomics* **2**, 1156 (Sep, 2002).
18. J. K. Eng, A. L. McCormack, J. R. Yates, *J Am Soc Mass Spectrom* **5**, 976 (1994).
19. B. Cooper, D. Eckert, N. L. Andon, J. R. Yates, P. A. Haynes, *J Am Soc Mass Spectrom* **14**, 736 (Jul, 2003).
20. W. J. Qian *et al.*, *J Proteome Res* **4**, 53 (Jan-Feb, 2005).
21. R. Craig, R. C. Beavis, *Bioinformatics* **20**, 1466 (Jun 12, 2004).
22. A. Keller, A. I. Nesvizhskii, E. Kolker, R. Aebersold, *Anal Chem* **74**, 5383 (Oct 15, 2002).
23. A. I. Nesvizhskii, A. Keller, E. Kolker, R. Aebersold, *Anal Chem* **75**, 4646 (Sep 1, 2003).

Supplemental Figure 1.

A.

FPA hardware loaded with top chamber containing either RNA fixative OR additional LB media

↓

Flight FPA group delivered to Space Shuttle and ground FPA group delivered to OES room in SLSL

↓

Space Shuttle launched and all FPA hardware identically activated at 9 days post-launch

↓

At 25 hours post-activation, all FPA cultures for RNA/protein analysis are fixed and all FPA cultures for virulence studies are supplemented with additional LB media

↓

Space Shuttle lands on day 12 post-launch and at 2.5 hours post-landing, flight FPA hardware recovered from Space Shuttle

↙ ↘

Flight and ground FPA cultures containing RNA/protein fixative are unloaded and frozen at -80 C

Flight and ground FPA cultures for virulence studies are unloaded and used in murine infection model

B.

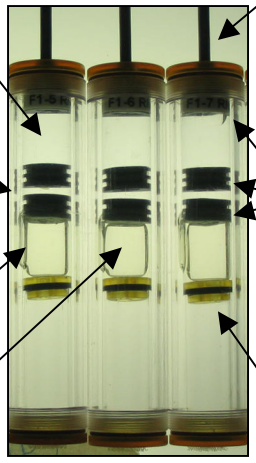

C.

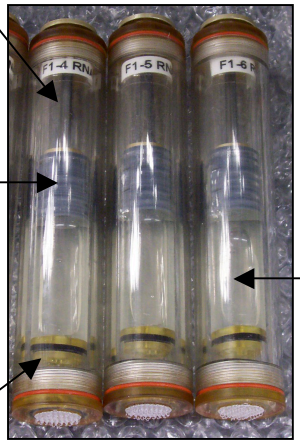

Supplemental Table 1: *Salmonella typhimurium* genes differentially-regulated during spaceflight mission STS-115

UP-regulated

Gene number	Fold change	Gene name	Known or putative function
Secreted proteins:			
STM1959	2.10	fliC	flagellar biosynthesis; flagellin, filament structural protein
STM2066	2.31	sopA	Secreted effector protein of Salmonella dublin
STM2883	2.57	sipD	cell invasion protein
STM2884	6.28	sipC	cell invasion protein
Membrane proteins:			
STM0374	2.04	yaiV	putative inner membrane protein
STM1070	2.05	ompA	putative hydrogenase, membrane component
STM1572	3.34	nmpC	new outer membrane protein; predicted bacterial porin
STM2267	2.44	ompC	outer membrane protein 1b (ib;c), porin
STM3420	3.12	secY	preprotein translocase of IISP family, putative membrane ATPase
Other function:			
STM0152	2.18	aceE	pyruvate dehydrogenase, decarboxylase component
STM0182	2.21	panB	3-methyl-2-oxobutanoate hydroxymethyltransferase
STM0240	2.02	yaeJ	putative-tRNA hydrolase domain
STM0272	2.36		putative ATPase with chaperone activity; homologue of Yersinia clpB
STM0596	2.24	entE	2,3-dihydroxybenzoate-AMP ligase
STM0730	4.75	gltA	citrate synthase
STM1040	2.12		Gifsy-2 prophage; probable minor tail protein
STM1290	7.67	gapA	glyceraldehyde-3-phosphate dehydrogenase A
STM1749	4.76	adhE	iron-dependent alcohol dehydrogenase of AdhE
STM2106	2.07	wcaI	putative glycosyl transferase in colanic acid biosynthesis
STM2118	2.30	wza	putative polysaccharide export protein, outer membrane
STM2181	2.06	yohJ	putative effector of murein hydrolase LrgA
STM2282	2.58	glpQ	glycerophosphodiester phosphodiesterase, periplasmic
STM2314	2.58		putative chemotaxis signal transduction protein
STM2708	2.03		Fels-2 prophage: similar to tail fiber protein (gpI) in phage P2
STM2719	2.12		Fels-2 prophage: similar to gpR in phage 186
STM2843	2.03	hydN	electron transport protein (FeS senter) from formate to hydrogen
STM2846	2.26	hycH	processing of HycE (part of the FHL complex)
STM2855	3.25	hypB	hydrogenase-3 accessory protein, assembly of metallocenter
STM4311	3.58	tnpA	IS200 transposase
STM4325	6.39	dcuA	Dcu family, anaerobic dicarboxylate transport protein
STM4415	2.71	fbp	fructose-bisphosphatase
STM4466	4.07		putative carbamate kinase
SSL_2286	2.97	orf36	putative phage replicase

Putative, unknown function:

STM0289	2.08		putative cytoplasmic protein
STM0699	2.76		putative cytoplasmic protein
STM2744	2.44		putative cytoplasmic protein
STM3752	2.05		putative cytoplasmic protein
SSL_T1747	4.06		putative cytoplasmic protein

Plasmid genes:

Plasmid 1 (pSLT):

PSLT011	2.20	srgA	sdiA-regulated gene; putative thiol-disulfide isomerase or thioredoxin
PSLT015	4.44	orf5	putative outer membrane protein
PSLT039	2.21	spvB	Salmonella plasmid virulence: hydrophilic protein
PSLT043	4.21		putative phosphoribulokinase / uridine kinase family
PSLT044	4.43		putative integrase protein
PSLT054	2.37	samB	mutagenesis by UV and mutagens; related to umuDC operon
PSLT068	2.04		putative ParB-like nuclease domain
PSLT072	2.11		putative transglycosylase
PSLT081	4.71	traB	conjugative transfer: assembly
PSLT095	4.24	traN	conjugative transfer: aggregate stability
PSLT099	2.32	trbB	conjugative transfer
PSLT100	2.59	traH	conjugative transfer: assembly
PSLT101	2.20	traG	conjugative transfer: assembly abd aggregate stability
PSLT104	2.87	traD	conjugative transfer: DNA transport
PSLT110	2.37	traX	conjugative transfer: fimbrial acetylation

Plasmid 2:

SSL_36	2.02	colIb	colicin Ib protein
SSL_T3	2.68	trbC	conjugative transfer
SSL_T5	3.14	trbA	conjugative transfer
SSL_T12	2.34	traT	conjugative transfer
SSL_T20	2.91	traK	conjugative transfer
SSL_T24	2.10	traF	conjugative transfer
SSL_T35	3.03	pilL	lipoprotein
SSL_T45	2.32	yagA	unknown function
SSL_T52	2.17	stbA	plasmid stability
SSL_T53	5.31	orf05	unknown function
SSL_T66	2.93	ygbA	unknown function

Plasmid 3:

SSL_T69	2.39	tnpB	putative transposase
SSL_T70	14.1	strB	streptomycin resistance
SSL_T71	3.55	strA	streptomycin resistance
SSL_T72	7.43	sulII	sulphonamide resistance
SSL_5085	2.08	repA	plasmid replication

DOWN-regulated

Protein secretion:

STM1153	0.342	msyB	suppresses protein export mutants
STM2895	0.417	invB	surface presentation of antigens; secretory proteins
STM3293	0.432	secG	preprotein translocase IISP family
STM3701	0.473	secB	molecular chaperone in protein export
STM3974	0.445	tatB	component of Sec-independent protein secretion pathway
STM4147	0.392	secE	preprotein translocase IISP family, membrane subunit

Flagella:

STM1916	0.458	cheY	chemotaxis regulator, transmits signals to flagelllar motor
STM1925	0.356	flhD	regulator of flagellar biosynthesis, acts on class 2 operons
STM1962	0.443	fliT	flagellar biosynthesis; possible export chaperone for FliD

Fimbrial:

STM0543	0.434	fimA	major type 1 subunit fimbrin (pilin)

Stress proteins:

STM0831	0.273	dps	stress response DNA-binding protein
STM1652	0.200	ynaF	putative universal stress protein

Regulatory:

STM_sRNA	0.458	RFN	putative small regulatory RNA
STM_sRNA	0.499	rne5	putative small regulatory RNA
STM_sRNA	0.318	csrB	regulatory RNA
STM0473	0.389	hha	hemolysin expression modulating protein
STM0606	0.493	ybdO	putative transcriptional regulator, LysR family
STM0959	0.415	lrp	regulator for lrp regulon (AsnC family)
STM1444	0.391	slyA	transcriptional regulator for hemolysin (MarR family)
STM1660	0.494	fnr	transcriptional regulator
STM2640	0.402	rpoE	sigma E (sigma 24) factor of RNA polymerase
STM3466	0.438	crp	catabolite activator protein (CAP), cyclic AMP protein (CRP family)
STM4315	0.445	rtsA	AraC-type DNA-binding domain-containing protein
STM4361	0.298	hfq	host factor I for bacteriophage Q beta replication

Ribosomal:

STM0216	0.344	rpsB	30S ribosomal subunit protein S2
STM0469	0.474	rpmE2	putative 50S ribosomal protein L31 (second copy)
STM2675	0.356	rimM	16S rRNA processing protein
STM3345	0.310	rplM	50S ribosomal subunit protein L13
STM3425	0.403	rplF	50S ribosomal subunit protein L6
STM3428	0.438	rplE	50S ribosomal subunit protein L5
STM3430	0.182	rplN	50S ribosomal subunit protein L14
STM3433	0.422	rplP	50S ribosomal subunit protein L16
STM3436	0.289	rpsS	30S ribosomal subunit protein S19
STM3438	0.457	rplW	50S ribosomal subunit protein L23
STM3439	0.393	rplD	50S ribosomal subunit protein L4, regulates S10 expression

STM3448	0.250	rpsL	30S ribosomal subunit protein S12
STM4150	0.423	rplA	50S ribosomal subunit protein L1, regulates L1 and L11
STM4391	0.401	rpsF	30S ribosomal subunit protein S6

Membrane/periplasmic proteins:

STM1164	0.340	yceB	putative outer membrane lipoprotein
STM1249	0.443		putative periplasmic protein
STM1432	0.464	ydhO	putative cell wall-associated hydrolase
STM1460	0.408	ydgK	putative inner membrane protein
STM1732	0.276	ompW	outer membrane protein W; colicin S4 receptor
STM1798	0.471	ycgR	putative inner membrane protein
STM2505	0.410		putative inner membrane protein
STM2685	0.411	smpA	small membrane protein A
STM2802	0.453	ygaM	putative inner membrane protein
STM2870	0.462		putative inner membrane protein
STM3107	0.460	yggN	putative periplasmic protein
STM3228	0.378	yqjC	putative periplasmic protein
STM3229	0.485	yqjD	putative inner membrane protein
STM3231	0.457	yqjK	putative inner membrane protein
STM3347	0.393	yhcB	putative periplasmic protein
STM4378	0.328	yjfN	putative inner membrane protein
STM4561	0.319	osmY	hyperosmotically inducible periplasmic protein

Other function:

STM0186	0.406	dksA	dnaK suppressor protein
STM0368	0.386	prpB	putative carboxyphosphonoenolpyruvate mutase
STM0369	0.403	prpC	putative citrate synthase
STM0417	0.382	ribH	riboflavin synthase, beta chain
STM0536	0.483	ppiB	peptidyl-prolyl cis-trans isomerase B (rotamase B)
STM0665	0.480	gltI	ABC superfamily (bind_prot), glutamate/aspartate transporter
STM0759	0.492	ybgS	putative homeobox protein
STM0803	0.408	moaB	molybdopterin biosynthesis, protein B
STM0966	0.497	dmsC	anaerobic dimethyl sulfoxide reductase, subunit C
STM1196	0.336	acpP	acyl carrier protein
STM1291	0.474	yeaA	putative peptide methionine sulfoxide reductase
STM1569	0.458	fdnH	formate dehydrogenase-N, Fe-S beta subunit, nitrate-inducible
STM1783	0.478	pth	peptidyl-tRNA hydrolase
STM2488	0.436	nlpB	lipoprotein-34
STM2542	0.495	nifU	NifU homologs involved in Fe-S cluster formation
STM2549	0.460	asrB	anaerobic sulfide reductase
STM2646	0.294	yfiD	putative formate acetyltransferase
STM2746	0.344		putative Excinuclease ATPase subunit
STM2767	0.491		putative Superfamily I DNA and RNA helicase
STM3039	0.455	idi	isopentenyldiphosphate isomerase
STM3054	0.431	gcvH	glycine cleavage complex protein H
STM3241	0.458	tdcE	pyruvate formate-lyase 4/ 2-ketobutyrate formate-lyase
STM3443	0.404	bfr	bacterioferrin, an iron storage homoprotein
STM3702	0.453	grxC	glutaredoxin 3

STM3703	0.321	yibN	putative Rhodanese-related sulfurtransferases
STM3870	0.484	atpE	membrane-bound ATP synthase, F0 sector, subunit c
STM3915	0.492	trxA	thioredoxin 1, redox factor
STM4341	0.411	frdC	fumarate reductase, anaerobic, membrane anchor polypeptide
STM4414	0.475	ppa	inorganic pyrophosphatase

Putative ORF, unknown function:

STM0474	0.435	ybaJ	putative cytoplasmic protein
STM1367	0.378	ydiH	putative cytoplasmic protein
STM1583	0.441		putative cytoplasmic protein
STM2390	0.290	yfcZ	putative cytoplasmic protein
STM2801	0.451	ygaC	putative cytoplasmic protein
STM3461	0.493		putative cytoplasmic protein
STM3654	0.341		pseudogene; in-frame stop following codon 23
STM3995	0.459	yihD	putative cytoplasmic protein
STM4002	0.172		putative cytoplasmic protein
STM4088	0.357	yiiU	putative cytoplasmic protein
STM4239	0.334		putative cytoplasmic protein
STM4240	0.411	yjbJ	putative cytoplasmic protein
STM4250	0.422	yjbQ	putative cytoplasmic protein
STM4499	0.494	yeeN	putative cytoplasmic protein

Supplemental Table 2: *Salmonella typhimurium* proteins identified in flight and ground total cell samples from STS-115 using MudPIT analysis (251 proteins total)

Protein name	Accession number	Protein molecular weight (Daltons)	Ground total cell protein ID probability*	Flight total cell protein ID probability*
aspartate ammonia-lyase	gi|16767575	52268.1	100%	100%
translation elongation factor EF-Tu.A	gi|96718	43233.6	100%	100%
elongation factor G	gi|16766735	77582	100%	100%
putative hydrogenase membrane component precursor	gi|16764429	37497.2	100%	100%
GroEL protein	gi|16767579	57267.8	100%	100%
30S ribosomal protein S1	gi|16764341	61154.4	100%	100%
L-asparaginase	gi|16766407	36908.5	100%	100%
phosphoenolpyruvate carboxykinase	gi|16766788	59559.8	100%	100%
enolase	gi|16766258	45468	100%	100%
glyceraldehyde 3-phosphate dehydrogenase A	gi|16764641	35568.6	100%	100%
periplasmic glycerophosphodiester phosphodiesterase	gi|16765609	40407.8	100%	100%
molecular chaperone DnaK	gi|16763402	69241.2	100%	100%
30S ribosomal protein S3	gi|16766723	25965.5	100%	100%
formate acetyltransferase 1	gi|16764333	84989.4	100%	100%
50S ribosomal subunit protein L7/L12	gi|16767406	12281	100%	100%
ribosomal protein S7	gi|16766736	17572.5	100%	100%
histone like DNA-binding protein HU-alpha (NS2) (HU-2)	gi|16767424	9503.1	100%	100%
glycerol kinase	gi|16767352	56046.2	100%	100%
dihydrolipoamide dehydrogenase	gi|16763544	50621.8	100%	100%
sn-glycerol-3-phosphate dehydrogenase	gi|16766813	56908.5	100%	100%
trigger factor	gi|16763828	48048.1	100%	100%
cold shock protein	gi|16765178	7384.3	100%	100%
DNA-binding protein HLP-II	gi|16765095	15525	100%	100%
ATP synthase beta subunit	gi|16767149	50265.5	100%	100%
phosphoglycerate kinase	gi|16766370	41115.1	100%	100%
iron-dependent alcohol dehydrogenase AdhE	gi|16765093	96199.8	100%	100%
50S ribosomal subunit protein L1	gi|16767404	24710.5	100%	100%
30S ribosomal protein S4	gi|16766705	23467.7	100%	100%
50S ribosomal subunit protein L13	gi|16766640	16000.7	100%	100%
putative outer membrane porin precursor	gi|16764916	39662.7	99%	99%
FKBP-type peptidyl-prolyl cis-trans isomerase	gi|16766742	28928.6	100%	100%
transketolase 1 isozyme	gi|16766377	72117	100%	100%
50S ribosomal subunit protein L5	gi|16766717	20300.6	100%	100%
DNA-directed RNA polymerase beta' subunit	gi|16767408	155220	100%	100%
30S ribosomal protein S13	gi|16766707	13144.1	100%	100%
alkyl hydroperoxide reductase C22 subunit	gi|16763985	20729.7	100%	100%
30S ribosomal subunit protein S5	gi|16766712	17585	100%	100%
50S ribosomal protein L24	gi|16766718	11298.3	100%	100%
DNA protection during starvation protein	gi|16764193	18699.8	100%	100%
ribosomal protein L19	gi|16765988	13112	100%	100%
acyl carrier protein	gi|16764551	8621.4	100%	100%
isocitrate dehydrogenase	gi|16764593	45771	100%	93%
triosephosphate isomerase	gi|16767347	26899	100%	100%
50S ribosomal subunit protein L3	gi|16766729	22228.7	100%	100%
30S ribosomal protein S2	gi|16763606	26741.2	100%	100%
lysine decarboxylase	gi|16765879	81220.5	100%	100%
putative universal stress protein	gi|16763991	15882.8	100%	100%
putative thiol-alkyl hydroperoxide reductase	gi|16763782	22299	100%	100%
50S ribosomal protein L9	gi|16767640	15765.8	100%	100%
50S ribosomal subunit protein L10	gi|16767405	17782.8	100%	100%
30S ribosomal subunit protein S16	gi|16765991	9216.7	100%	100%
50S ribosomal protein L20	gi|16764687	13479.6	100%	100%
pyruvate kinase	gi|16764728	50639.5	100%	98%
6-phosphogluconate dehydrogenase	gi|16765411	51379.2	100%	93%
inorganic pyrophosphatase	gi|16767660	19658.8	100%	100%
50S ribosomal protein L4	gi|16766728	22068.6	100%	100%
50S ribosomal protein L11	gi|16767403	14857.5	100%	100%
50S ribosomal subunit protein L17	gi|16766703	14377.2	100%	100%

succinyl-CoA synthetase beta chain	gi|16764108	41462.8	100%	100%
50S ribosomal subunit protein L6	gi|16766714	18841.3	100%	100%
fructose 1,6-bisphosphate aldolase	gi|16766369	39138.4	100%	100%
aconitate hydratase 2	gi|16763548	93513.7	100%	100%
iron superoxide dismutase	gi|16764779	21290.4	100%	100%
50S ribosomal protein L22	gi|16766724	12208.6	100%	100%
sn-glycerol-3-phosphate dehydrogenase large subunit	gi|16765611	59039.6	100%	100%
RNA polymerase, alpha subunit	gi|16766704	36494.1	100%	100%
30S ribosomal protein S10	gi|16766730	11748.8	100%	100%
RNA polymerase, beta subunit	gi|16767407	150586.6	100%	99%
polynucleotide phosphorylase	gi|16766580	77020.9	100%	100%
Lpp1 murein lipoprotein	gi|16764727	8373.6	100%	93%
malate dehydrogenase	gi|16766654	32457.8	100%	100%
citrate synthase	gi|16764100	48089.9	100%	100%
GroES protein	gi|16767578	10300.1	100%	100%
putative glutamic dehyrogenase-like protein	gi|16765136	48020.6	100%	100%
succinyl-CoA synthetase alpha subunit	gi|16764109	29757.8	99%	100%
transaldolase B	gi|16763397	35154.5	100%	100%
glycine dehydrogenase	gi|16766354	104270.1	93%	100%
transcription elongation factor NusA	gi|16766585	55408.3	100%	100%
flagellar biosynthesis filament structural protein	gi|16766083	52518.5	100%	100%
elongation factor Ts	gi|16763607	30339.6	100%	100%
N-acetylneuraminate lyase	gi|16766634	32437.7	100%	100%
50S ribosomal subunit protein L32	gi|16764546	6428.4	100%	100%
ATP synthase alpha subunit	gi|16767151	55096	100%	97%
50S ribosomal subunit protein L14	gi|16766719	13550.2	99%	100%
phosphate acetyltransferase	gi|16765792	82305.8	100%	100%
50S ribosomal subunit protein L15	gi|16766710	14948.9	100%	100%
ribose-phosphate pyrophosphokinase	gi|16765121	34198.6	100%	88%
hydrogenase-2 large subunit	gi|16766447	62420.6	100%	100%
cytoplasmic ferritin	gi|16765276	19262.5	100%	100%
riboflavin synthase subunit beta	gi|16763797	15990.5	100%	97%
50S ribosomal subunit protein L29	gi|16766721	7242.6	100%	93%
putative universal stress protein	gi|16764996	15696.7	93%	100%
periplasmic nitrate reductase	gi|16765587	92856.9	100%	93%
hyperosmotically-inducible periplasmic protein	gi|16767802	21430.3	93%	93%
ornithine carbamoyltransferase	gi|16767710	36798.4	100%	100%
30S ribosomal protein S11	gi|16766706	13812.8	100%	100%
formate dehydrogenase alpha subunit	gi|16767302	112357.4	100%	100%
nucleoside diphosphate kinase (ndk)	gi|16765846	15503.7	100%	100%
putative pyruvate-flavodoxin oxidoreductase	gi|16764995	128563.7	55%	100%
glycoprotein/polysaccharide metabolism protein	gi|16763846	19458.9	100%	100%
O-acetyl serine sulfhydrylase	gi|11514514	34414.7	93%	100%
30S ribosomal subunit protein S21	gi|16766509	8482.1	100%	100%
ornithine decarboxylase isozyme	gi|16764071	82432.6	100%	99%
fumarate reductase	gi|16767591	27157.3	100%	100%
anaerobic glycerol-3-phosphate dehydrogenase subunit B	gi|16765612	45653.3	100%	100%
glucose-specific PTS system enzyme IIA component	gi|16765753	18229.5	100%	100%
DNA-directed RNA polymerase omega subunit	gi|16767026	10218.3	100%	100%
FKBP-type peptidyl-prolyl cis-trans isomerase	gi|16766744	20767.9	100%	100%
pyruvate dehydrogenase E1 component	gi|16763542	99564	100%	97%
phosphate acetyltransferase	gi|16765665	77261.1	100%	93%
glucose-6-phosphate isomerase	gi|16767471	61412.3	100%	93%
putative oxidase	gi|16764715	113118.3	93%	99%
50S ribosomal subunit protein L16	gi|16766722	15176.6	100%	100%
enterobactin synthetase component F	gi|16763965	141727.2	78%	99%
50S ribosomal subunit protein L2	gi|16766726	29802.1	93%	100%
acetyl-coenzyme A carboxylase subunit alpha	gi|16763622	35327.3	100%	59%
pyruvate kinase	gi|16765230	51369.5	100%	93%
serine hydroxymethyltransferase	gi|16765875	45437	100%	93%
50S ribosomal subunit protein L28	gi|16767013	9032.6	93%	93%
isoaspartyl dipeptidase	gi|16767756	40306.8	100%	93%
sensory histidine kinase	gi|16765598	106264.3	100%	79%
putative inner membrane lipoprotein	gi|16765852	179631.1	87%	87%
Initiation factor IF-3	gi|16419853	16619.9	100%	100%

putative protease	gi|16764427	65586.3	99%	97%
thiosulfate reductase electron transport protein PhsB	gi|16765394	21300.7	93%	100%
dihydrolipoamide acetyltransferase	gi|16764107	43839.8	100%	100%
protein-export protein SecB	gi|16766986	17227	100%	100%
cytochrome d terminal oxidase polypeptide subunit I	gi|16764110	58299.5	100%	100%
putative detox protein in ethanolamine utilization	gi|16765785	9824.4	100%	100%
galactose transport protein	gi|16765520	35796.1	100%	99%
putative translation initiation inhibitor	gi|16767703	13557.2	100%	93%
dihydrolipoamide acetyltransferase	gi|16763543	66121.5	100%	93%
glutamine ABC transporter periplasmic-binding protein	gi|16764192	27245.6	93%	93%
putative selenocysteine synthase	gi|16767692	39874.5	47%	93%
30S ribosomal protein S20	gi|16763433	9637.9	100%	93%
NADH dehydrogenase I chain G	gi|16420864	100254.5	100%	100%
acetyl-CoA carboxylase	gi|16766675	49245.8	99%	100%
RNase E	gi|16764541	119381.7	100%	100%
fructose-1,6-bisphosphatase	gi|16767661	36781.5	100%	100%
phosphoenolpyruvate synthase	gi|16764700	87191.6	100%	100%
putative formate acetyltransferase	gi|16765966	14326.2	100%	93%
lipoprotein	gi|16765808	36919.8	100%	93%
sensory transduction histidine kinase	gi|16764736	65221.8	93%	54%
sensory kinase in two-component system with CreB	gi|16767830	51666.7	93%	59%
agmatinase	gi|16766379	33585.5	100%	100%
aminoacyl-histidine dipeptidase	gi|16763698	52419.9	93%	100%
30S ribosomal subunit protein S19	gi|16766725	10398.5	100%	93%
glucose-1-phosphate adenylyltransferase	gi|16766822	48444.5	100%	83%
acetate kinase	gi|16765664	43240.3	100%	92%
ABC superfamily peptide transport protein	gi|16765039	30654.8	48%	100%
potassium-transporting ATPase subunit B	gi|16764075	72125	99%	74%
adenylosuccinate synthetase	gi|16767612	47359.7	100%	100%
ATP synthase delta subunit	gi|16767152	19394.2	97%	100%
glycerol dehydrogenase	gi|16767374	38723.5	100%	96%
succinate dehydrogenase catalytic subunit	gi|16764105	26847.2	100%	93%
FkbP-type peptidyl-prolyl cis-trans isomerase	gi|16767643	23719.2	100%	93%
putative sigma(54) modulation protein	gi|16765980	12634.6	100%	93%
ATP synthase epsilon subunit	gi|16767148	15046.6	100%	93%
putative cytoplasmic protein	gi|16765717	10269.4	100%	93%
needle complex major subunit PrgI	gi|16766179	8839.3	93%	100%
cytochrome o ubiquinol oxidase subunit I	gi|16763823	74265.7	93%	100%
fumarate reductase, flavoprotein subunit	gi|16767592	65473.9	93%	100%
putative lipoprotein	gi|16764058	12218.6	72%	96%
phase 1 flagellin	gi|16765297	51594.5	100%	100%
transcription termination factor Rho	gi|16767192	46977.2	100%	100%
arginine deiminase	gi|16767712	45544.5	99%	100%
serine endoprotease	gi|16766643	47310.1	93%	100%
putative fructose-1,6-bisphosphate aldolase	gi|16767344	31725.2	93%	100%
NADH dehydrogenase I chain F	gi|16765651	49229.2	100%	93%
small membrane protein A	gi|16766000	12327	93%	100%
single-strand DNA-binding protein	gi|16767506	19055.5	93%	100%
aldehyde oxidoreductase	gi|3885918	49239.5	93%	100%
PilQ ATP-binding protein	gi|32470257	58267.7	98%	86%
BipA GTPase	gi|16767274	67359.4	100%	66%
TrpR binding protein WrbA	gi|16764477	20849.7	100%	93%
catalase HPII	gi|16764669	83610.2	93%	100%
ethanolamine utilization protein EutL	gi|16765776	22678	100%	81%
nikB plasmid protein	gi|20521580	103992.3	79%	100%
thioredoxin	gi|16767191**	11789.4	100%	0
aldose 1-epimerase	gi|16764640	32541.6	100%	0
phosphopentomutase	gi|16767810	44227.1	100%	0
D-ribose-binding protein	gi|1070661	28512.8	93%	0
oriT nickase/helicase	gi|16445291	191664	100%	0
DNA polymerase I	gi|16767264	103114.9	93%	0
ATPase subunit	gi|7594817	46171.1	100%	0
phosphoglyceromutase	gi|16766989	56237.5	100%	0
putative periplasmic protein	gi|16765796	38706.3	100%	0
inositol-5-monophosphate dehydrogenase	gi|16765831	51930.1	100%	0

putative ATP-dependent helicase	gi|16765162	70268.1	93%	0
hydrogenase 3 large subunit	gi|16766155	65003.1	100%	0
mannose-specific enzyme IIAB	gi|16765171	34969.2	100%	0
30s ribosomal protein S6	gi|16767637**	15154.9	100%	0
dipeptide transport protein	gi|16766917	60202.5	100%	0
D-fructose-6-phosphate amidotransferase	gi|16767145	66860.7	100%	0
tetrathionate reductase subunit A (TtrA)	gi|16764733	110976.9	97%	0
uridine phosphorylase	gi|16422527	27205.9	100%	0
anaerobic dimethyl sulfoxide reductase chain B	gi|16764326**	22761.6	100%	0
virulence-associated protein mkfB	gi|7443056	62570.6	100%	0
prolyl-tRNA synthetase	gi|16763631	63522.6	100%	0
cytosine deaminase	gi|16766629	47608	100%	0
ribosome recycling factor	gi|16763609	20538	100%	0
dihydrodipicolinate synthase	gi|16765809**	31276.4	100%	0
putative dehydrogenase	gi|16765715	77238.8	99%	0
outer membrane-bound fatty acid transporter	gi|16765718	47688.5	93%	0
putative cytoplasmic protein	gi|16763672**	79560.5	99%	0
2-dehydro-3-deoxyphosphooctonate aldolase	gi|16765113	30777.4	93%	0
periplasmic maltose-binding protein	gi|16767479	43468	100%	0
chemotactic response protein	gi|16765257**	23902.4	100%	0
putative acetyltransferase	gi|16765805	74000	100%	0
phosphoglucosamine mutase	gi|16766590	47424.2	100%	0
ATP-dependent RNA helicase	gi|16765963	50040.2	100%	0
glutamine synthetase	gi|16767272	51768.7	100%	0
outer membrane protein Tsx	gi|16763793	32761.5	100%	0
ribonuclease R (RNase R)	gi|16767614	92033.1	99%	0
DNA-binding protein HU-beta	gi|16763832	9222	99%	0
putative zinc-binding dehydrogenase	gi|16764887	37229	100%	0
transcriptional repressor for rbs operon (GalR/LacI family)	gi|16767170	36702.1	100%	0
ubiquinone/menaquinone methyltransferase UbiE	gi|16767240	28118.9	100%	0
phosphoheptose isomerase	gi|16763693	20878.5	100%	0
ClpB ATP-dependent protease	gi|16765976	95421.8	99%	0
putative pyrophosphatase	gi|16766260	30812.9	99%	0
putative GTP-binding protein	gi|16766597	43086.7	99%	0
putative 5'-nucleotidase/2',3'-cyclic phosphodiesterase	gi|16767370	56560	98%	0
hypothetical ABC transporter ATP-binding protein	gi|16763887	24467.3	98%	0
putative glycosyl transferase	gi|16765625	36500	98%	0
citrate lyase alpha chain	gi|56967225	54561.7	97%	0
arginine-binding periplasmic protein 1 precursor	gi|16764251	26979.4	0	93%
cold shock-like protein cspE	gi|16764006	7433.5	0	93%
outer membrane protein C	gi|16765595**	41222.1	0	93%
lysine decarboxylase 2	gi|16763624	80747.8	0	93%
putative integral membrane protein	gi|16764196	59589.3	0	93%
aminopeptidase B	gi|16765856	46339	0	93%
glycerate kinase II	gi|16763905	39003.1	0	99%
ecotin precursor	gi|16765590	18199.7	0	100%
3,4-dihydroxy-2-butanone 4-phosphate synthase	gi|16766495	23292.3	0	86%
2-oxoglutarate dehydrogenase	gi|16764106	104805.9	0	100%
D-ribose-binding periplasmic protein	gi|16767168	30944.8	0	99%
flagellar hook-associated protein	gi|16765298	49818.7	0	87%
cysteine desulfurase	gi|16765863	45075.7	0	83%
hydrogenase-3 accessory protein	gi|16766161**	31375.2	0	99%
putative imidazolonepropionase or amidohydrolase	gi|16767659	42408	0	100%
asparagine synthetase B	gi|16764050	62555.9	0	100%
50S ribosomal subunit protein L30	gi|16766711**	6495.8	0	100%
50S ribosomal subunit protein L23	gi|16766727**	11194.9	0	100%
membrane-bound ATP synthase, epsilon-subunit	gi|6625704	14848.1	0	100%
hydrogenase-2 small chain protein	gi|16766450	39604.2	0	100%
ATP synthase subunit C	gi|16767150	31538	0	100%
precorrin-8X methylmutase	gi|16765363	23016.8	0	99%
translation initiation factor IF-2	gi|16766584	97383.5	0	99%
ethanolamine ammonia-lyase heavy chain	gi|16765778	49432	0	99%
putative copper-transporting ATPase	gi|16763878	87893	0	99%

*Peptide samples obtained from MudPIT were analyzed using Sequest and X!Tandem software, and the data was organized using the Scaffold program. To be considered a positive identification in Scaffold, the following parameters were used: a minimum of 2 peptides from a given protein identified with peptide and protein thresholds of 80% to give an overall protein identification (ID) probability of at least 80%. Note that a protein ID probability of greater than 80% in at least one of the samples warranted inclusion in the table so as to allow identification of possible differential expression of a given protein.

**Proteins identified via MuDPIT analysis as differentially expressed that also displayed differential expression via microarray analysis.